This document is confidential and is proprietary to the American Chemical Society and its authors. Do not copy or disclose without written permission. If you have received this item in error, notify the sender and delete all copies.

Thermal Percolation in Well-Defined Nanocomposite Thin Films

Manuscript ID Manuscript Type: Date Submitted by the Author: Complete List of Authors: Chang, Boyce; University of California Berkeley, Materials Science and Engineering Li, Chen; Cornell University, Mechanical and Aerospace Engineering Dai, Jinghang; Cornell University of California Berkeley, Chemistry Huang, Jingyu; University of California Berkeley, Materials Science and Engineering He, Mengdi; University of California Berkeley, Materials Science and Engineering Hu, Weili; University of California Berkeley, Chemistry Tian, Zhiting; Cornell University, Mechanical and Aerospace Engineering Xu, Ting; University of California Berkeley, Materials Science and Engineering	Journal:	ACS Applied Materials & Interfaces
Date Submitted by the Author: Complete List of Authors: Chang, Boyce; University of California Berkeley, Materials Science and Engineering Li, Chen; Cornell University, Mechanical and Aerospace Engineering Dai, Jinghang; Cornell University, Mechanical and Aerospace Engineering Evans, Katherine; University of California Berkeley, Chemistry Huang, Jingyu; University of California Berkeley, Materials Science and Engineering He, Mengdi; University of California Berkeley, Materials Science and Engineering Hu, Weili; University of California Berkeley, Chemistry Tian, Zhiting; Cornell University, Mechanical and Aerospace Engineering Xu, Ting; University of California Berkeley, Materials Science and	Manuscript ID	am-2022-00296t.R1
Author: Complete List of Authors: Chang, Boyce; University of California Berkeley, Materials Science and Engineering Li, Chen; Cornell University, Mechanical and Aerospace Engineering Dai, Jinghang; Cornell University, Mechanical and Aerospace Engineering Evans, Katherine; University of California Berkeley, Chemistry Huang, Jingyu; University of California Berkeley, Materials Science and Engineering He, Mengdi; University of California Berkeley, Materials Science and Engineering Hu, Weili; University of California Berkeley, Chemistry Tian, Zhiting; Cornell University, Mechanical and Aerospace Engineering Xu, Ting; University of California Berkeley, Materials Science and	Manuscript Type:	Article
Engineering Li, Chen; Cornell University, Mechanical and Aerospace Engineering Dai, Jinghang; Cornell University, Mechanical and Aerospace Engineering Evans, Katherine; University of California Berkeley, Chemistry Huang, Jingyu; University of California Berkeley, Materials Science and Engineering He, Mengdi; University of California Berkeley, Materials Science and Engineering Hu, Weili; University of California Berkeley, Chemistry Tian, Zhiting; Cornell University, Mechanical and Aerospace Engineering Xu, Ting; University of California Berkeley, Materials Science and		n/a
	Complete List of Authors:	Engineering Li, Chen; Cornell University, Mechanical and Aerospace Engineering Dai, Jinghang; Cornell University, Mechanical and Aerospace Engineering Evans, Katherine; University of California Berkeley, Chemistry Huang, Jingyu; University of California Berkeley, Materials Science and Engineering He, Mengdi; University of California Berkeley, Materials Science and Engineering Hu, Weili; University of California Berkeley, Chemistry Tian, Zhiting; Cornell University, Mechanical and Aerospace Engineering Xu, Ting; University of California Berkeley, Materials Science and

SCHOLARONE™ Manuscripts

Thermal Percolation in Well-Defined Nanocomposite Thin Films

Boyce S. Chang[†], Chen Li[‡], Jinghang Dai[‡], Katherine Evans^, Jingyu Huang[†], Mengdi He[†], Weili Hu^, Zhiting Tian[‡]*, Ting Xu^{†∧§}*

†Department of Materials Science and Engineering, University of California, Berkeley, Berkeley, California 94720, USA

^Department of Chemistry, University of California, Berkeley, Berkeley, California 94720, USA ‡Sibley School of Mechanical and Aerospace Engineering, Cornell University, Ithaca, New York 14853, USA

§Materials Science Division, Lawrence Berkeley National Laboratory, Berkeley, California 94720, USA

*tingxu@berkeley.edu, *zhiting@cornell.edu

||Equal contribution

Keywords: Nanocomposite, thermal transport, percolation, self-assembly, transient thermal grating, block copolymer

Abstract

Thermal percolation in polymer nanocomposites — the rapid increase in thermal transport due to the formation of networks among fillers — is the subject of great interest in thermal management ranging from general utility in multifunctional nanocomposites to high conductivity applications such as thermal interface materials. It remains, however, a challenging subject encompassing both experimental and modelling hurdles. Successful reports of thermal percolation are exclusively found in high aspect ratios, conductive fillers such as graphene, albeit at filler loadings significantly higher than the electrical percolation threshold. This anomaly was attributed to the lower filler-matrix thermal conductivity contrast ratio $k_f/k_m \sim 10^4$ compared to electrical conductivity $\sim 10^{12}$ - 10^{16} . In a randomly dispersed composite, the effect of low contrast ratio is further accentuated by uncertainties on the morphology of the percolating network and presence of other phases such as disconnected aggregates and colloidal dispersions. Thus, the general properties of percolating networks are convoluted as they lack defined structure. In contrast, a prototypical system with controllable nanofiller placement enables the elucidation of structureproperty relations such as filler size, loading and assembly. Using self-assembled nanocomposites with controlled 1,2,3-dimension nanoparticle (NP) arrangement, we demonstrate that thermal percolation can be achieved in spite of using spherical, non-conductive fillers (k_{l}/k_{m} ~60) at low volume fraction (9 vol%). We observe that the effects of volume fraction, interfacial thermal resistance and filler conductivity on thermal conductivity depart from effective medium approximations. Most notably, contrast ratio plays a minor role in thermal percolation above k_f/k_m ~60—a common range for semiconducting nanoparticles/polymer ratio. Our findings bring new perspective and insights to thermal percolation in nanocomposites, where the limits in contrast ratio, interfacial thermal conductance and filler size are established.

Introduction

Multi-functional polymer nanocomposites have garnered considerable attention due to its alluring properties and potential tunability. 1-3 Furthermore, the assembly of nanofillers dispersed in the polymer matrix serves as an additional design handle that could potentially unlock emergent properties such as plasmonic resonance, high strength composites and supercapacitors for energy storage.⁴⁻⁶ More recently, interest in the thermal transport properties of nanocomposites⁷⁻⁹ have dramatically increased due to the importance of thermal management across various fields such as microelectronics¹⁰, insulation¹¹ and thermoelectrics.¹²⁻¹³ While the subject has been rigorously studied, only few reports can be found on thermal percolation—the formation of networks among fillers followed by substantial increase in thermal conductivity. In fact, the very existence of thermal percolation in nanocomposites is a subject of debate, highlighted by conflicting reports on the absence and presence of thermal percolation in nanofillers. 14-15 Furthermore, thermal percolation has only been observed in highly conductive fillers such as graphene and hexagonal boron nitride (hBN) where the thermal conductivity ratio (contrast) between filler and matrix is relatively high (k_f/k_m~10⁵), albeit insignificant compared to electrical conductivity ratio $(k_f/k_m \sim 10^{15})$, in graphere fillers) where percolation effects has been widely observed. ¹⁶⁻¹⁹ The reported thermal percolating threshold varies between 17-30 vol%, which is unusually large for such high aspect ratio fillers. Electrical thresholds on the other hand, occur between 5-10 vol%. We hypothesize that the randomly dispersed composites have insufficient percolating networks to significantly boost thermal transport despite surpassing the electrical threshold. Furthermore, effective thermal conductivity becomes convoluted by the mixture of phases including filler networks, disconnected aggregates, and colloidal dispersions. Unlike their electrical counterpart,

the contribution of each phase to heat transfer is non-negligible. As a result, the lack of uniform morphology renders structure-property relationships including the effect of contact resistance challenging to resolve in percolating composites. 14, 20 Moreover, thermal percolation is becoming relevant in the general case—moderately conductive and spherical fillers—with the advent of multifunctional composites.

To systematically study thermal percolation in polymer nanocomposites, a self-assembling matrix that could uniformly direct spatial distribution of the nanoparticles (NP) is required. Block copolymer-based supramolecular nanocomposites have been extensively investigated to gain control over NP assemblies. They serve as ideal model systems for developing structure-property relations. Well-defined assembly of nanofillers in 1,2 and 3 dimensions have been demonstrated in the bulk and thin films of supramolecular nanocomposites. ²¹⁻²² The interface between NPs and polymer matrix can be mediated by small molecules hydrogen bonded to the chain side groups or dispersed in each microdomain to render chemical compatibility. Furthermore, the overall structure of the nanocomposite can be modulated by varying the supramolecule morphology and kinetic control via solvent annealing condition. ²³⁻²⁵

Here, we demonstrate thermal percolation in nanocomposites with spherical, non-conductive NPs (Fe₃O₄) and low filler loading—below theoretical limit for spherical fillers—using a bottom-up fabrication approach. Laser induced transient thermal grating (TTG) was employed to study the interactions between NP size, loading and assembly on the thermal percolation behavior of supramolecular nanocomposite thin films fabricated on quartz wafers (Figure 1). Interestingly, effective medium approximation (EMA) models were unable to describe the thermal transport behavior beyond the percolating threshold despite accounting for size/interfacial effects. Instead, thermal circuit analysis, which are designed for ideal systems successfully explained the

trends observed. Furthermore, the effects of volume fraction, interfacial thermal resistance, and filler conductivity on thermal transport deviate from traditional EMA-bound composites. Most notably, filler size effects play a more significant role in percolating nanocomposites as it scales directly with the number of filler-filler interfaces within each network compared to a randomly dispersion.

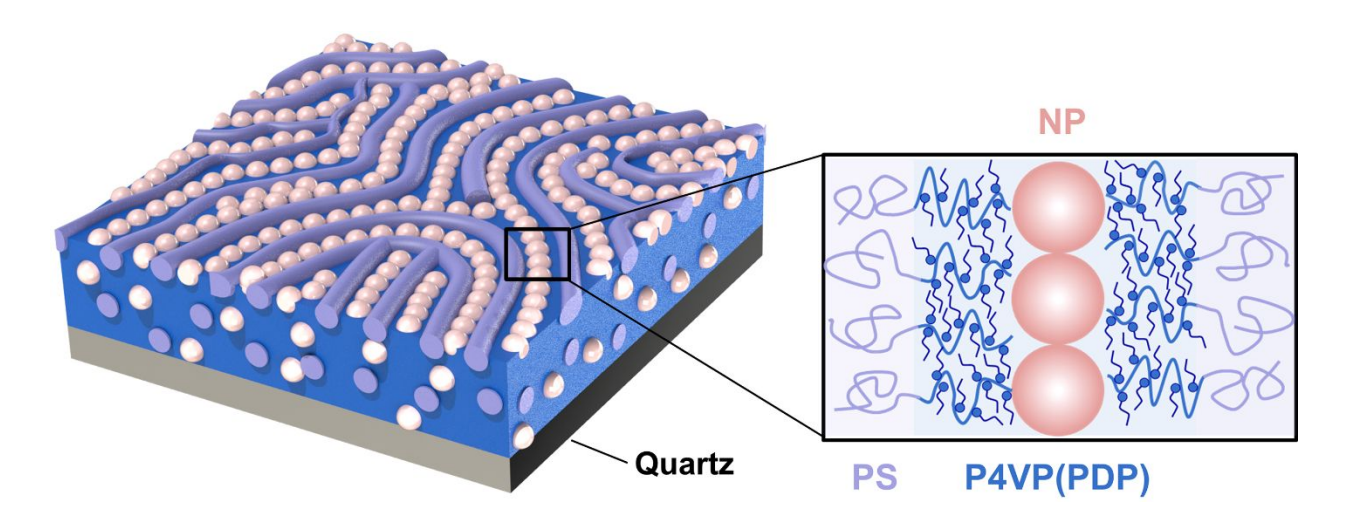


Figure 1. Schematic of bottom-up assembled block copolymer-based supramolecular nanocomposite. The supramolecule self-assembles into a cylindrical morphology isolating the nanoparticles (NP) to form a percolating network within the P4VP(PDP) domain.

Results and discussion

Thin films of well-defined nanocomposites were fabricated by spin coating a mixture of the iron oxide nanoparticles (NP) capped with oleic acid ligands and the supramolecular matrix, and subjected to solvent vapor annealing. The supramolecule consist of polystyrene-block-poly(4-vinylpyridine), PS-b-P4VP and 3-pentadecylphenol, PDP at a molar ratio of 1.7:1 with the pyridine

groups. Majority of the PDP occupies the pyridine sites in solution via hydrogen bonding while the remaining excess acts as a plasticizer that facilitates self-assembly. $^{26-27}$ PS(19,000 Da)-P4VP(5,200 Da)(PDP)_{1.7} (Lateral periodicity, L = 30nm) 22 was selected as the self-assembling matrix owing to its extensive structural diversity where morphological control of NPs ranging from 5-25 nm has been demonstrated. $^{23-25,28}$ Iron oxide nanoparticles (NP) were used as non-conductive nanofillers to leverage their absorption at wavelengths below 560 nm to facilitate the formation of thermal gratings used for TTG measurements. 29 Furthermore, these particles have been incorporated into block copolymer matrices to fabricate superparamagnetic thin films. 30 Despite local heat generation at the NPs, these processes occur on the order of ps while the decay of thermal gratings used for thermal diffusivity calculation are tracked on the order of μ s. Furthermore, the stable and clear thermal decay of these gratings indicate that the initial non-uniform heat distribution is negligible in these measurements (Figure S9).

Here, nanocomposites were confined to a filler volume percent, φ between 3-12 vol% in order to: i) achieve 3D NP assembly and ii) prevent kinetically trapped states caused by NP jamming.²⁴ The thin films were solvent annealed in chloroform vapor to aid self-assembly by boosting mobility of the supramolecule matrix. The extend of annealing is quantified through the change in thickness of the film, hence, the volume of solvent uptake.²³ The volume fraction of solvent, *f* (Details of calculation provided in the supporting information section S2) for this dataset was fixed at 0.62 to ensure equilibrated morphologies are obtained and the NPs are selectively incorporated in the P4VP(PDP) microdomains.²³ Atomic force microscopy (AFM) was used to study the morphological evolution of the films. The bright spheres represent NPs while dark and lighter matrix phases are P4VP(PDP) and PS domains, respectively (Figure 2a-d). As φ increased, the interparticle distance within P4VP(PDP) decreases and the population of particles visible on

the surface concomitantly multiplied. At 9 vol%, the NPs begin to form a chain-like network (Figure 2c), consistent with previous observations.²³ This observation is paired with a plateau in both interparticle distance (~20 nm) and NP surface coverage, indicating a saturation of NPs (Figure 2e). Details of image processing are provided in the supporting information section S2. At 12 vol% the nanocomposite becomes kinetically trapped²⁴, thus, exhibits a distorted network morphology (Figure 2d). With the addition of nanoparticles, the effective periodicity appears to be ~45 nm. Detailed studies on the structure of the nanocomposite have been reported previously.²², 31-33

Thermal transport measurements were conducted using TTG, where thermal diffusivity of the sample is extrapolated from the decay curve of a laser induced temperature grating over time.²⁹ Thermal conductivity, k is then obtained by multiplying diffusivity with volumetric heat capacity. At low φ (3-6 vol%), k plateaued at 0.55-0.56 W/m K (\pm 0.02). We note that these values are larger than previous reports on iron oxide composites with similar φ (0.3-0.4 W/m K).³⁴⁻³⁵ The disparities might arise from uncertainties in the heat capacity of the system and substrate effects in thin films.³⁶ After taking into account the substrate contribution, k of the sample could be approximately half of the reported value, making it comparable to literature. Despite the difference in absolute values, the offset is systematic and the trend across different samples stays the same. The detailed analysis on the contribution of substrate effect to the thermal conductivity is shown in the supporting information section S6. A transition occurs at φ =6-9 vol%, whereby a step increase from 0.56 to 0.81 W/m K (\pm 0.02) was observed. In conjunction with the chain-like assembly of NPs (Figure 2c), this behavior further suggests a classical percolation of fillers where the composite exhibits rapid increase in k at the critical threshold volume, φ * (Figure 2f).³⁷⁻³⁸

The same behavior was observed for both 10.7 nm and 20.4 nm NPs with similar morphology, albeit with the latter exhibiting a greater enhancement in thermal conductivity (Figure S2). A larger number of interparticle interfaces in 10.7 nm NPs could dampen the effects of thermal percolation due to interfacial thermal resistance. Similarly, phonon boundary scattering could play a role at such dimensions, however, this is unlikely the case considering the mean free path of Fe_3O_4 is ~1 nm (estimated from kinetic theory). In contrast to random polymer composites, ^{8, 39} percolation in supramolecular nanocomposites is organized into a uniform morphology throughout the film and occurs at a significantly lower φ due to matrix-guided assembly of the NPs.²⁴

Since we are most interested in the trend of the thermal conductivity change, normalized thermal conductivities were used with respect to 3 vol%, and the data was compared to EMA models such as Maxwell-Garnett and Hasselman-Johnson model, which is an extended EMA that accounts for filler size effects and interfacial thermal conductance, $h.^{40}$ The general EMA developed by Nan et al.⁴¹ reduces to the Hasselman-Johnson model in the case of spherical fillers. Thermal conductivity of the supramolecular matrix was not used in normalization because it is transparent to the excitation beam. We observe that both models corroborate with the data at low concentration (ϕ =3-6 vol%) but substantially under predicts above the ϕ * (Figure 2g). Agreement with the model suggests that heat transfer was initially matrix dominated as expected for non-percolating systems.

At the critical concentration, the NPs packs within the comb-block to form a network, which acts as thermal shortcuts in a parallel circuit. The percolating threshold, ϕ^* of spherical fillers in a well-defined nanocomposite reported in this work occurs at significantly lower concentrations (9 vol%) compared to a randomly distributed composite (39-47 vol%).⁴² Note that the theoretical minimum for randomly dispersed spherical fillers to achieve percolation is 16

vol%.³⁷ Interestingly, the Lewis-Nielsen model, which was successful in describing percolation in randomly dispersed graphene nanocomposites,¹⁷ similarly underpredicts the thermal conductivity of the self-assembled nanocomposite (Figure 2g). This is because the model was derived for percolation in random dispersions, which occur at much higher φ^* as described above.

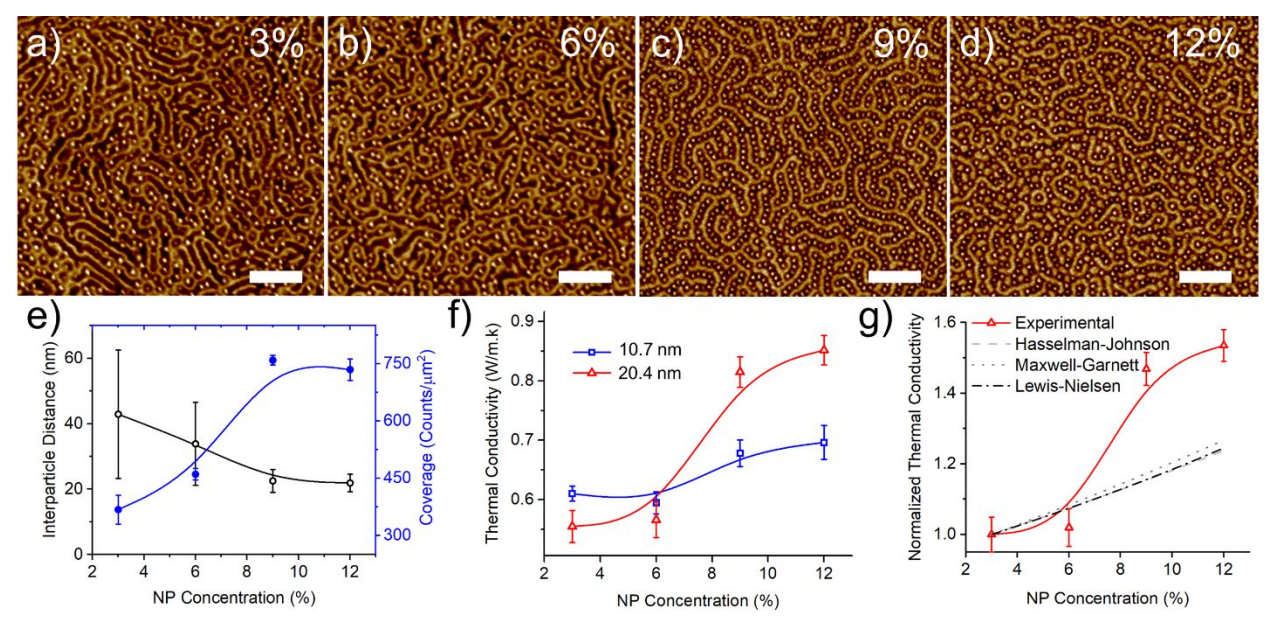


Figure 2. Morphology and thermal conductivity of a percolating nanocomposite through self-assembly. a-d) AFM images of nanocomposites with 20.4 nm NPs at various concentrations. Nanocomposite lateral periodicity, L = 45nm (Scale bar=200nm). E) Average interparticle distance and NP surface coverage from image processing of AFM images, and f) thermal conductivity as a function of NP concentration. g) Normalized thermal conductivity with respect to 3 vol% compared to effective medium approximation by Maxwell-Garnett and the inclusion size corrected Hasselman-Johnson model. Solid lines are drawn as a guide to the eye.

In order to demonstrate that percolation occurs throughout the film, the morphology of supramolecular nanocomposite was modulated at constant composition by leveraging kinetically

trapped states during solvent annealing.²⁸ Maintaining NP concentration at 9 vol% (above percolating threshold), nanocomposites annealed at different solvent fraction, f, were fabricated to reveal the effect of NP surface coverage on thermal conductivity (Figure 3a-b, Figure S3). During solvent annealing, NPs diffuse to the surface of the film due to entropic penalties associated with limited chain conformations at the matrix-filler interface.²⁸ This dataset is compared to the previous dataset where changes in surface coverage was observed due to φ with fixed annealing, f=0.62 (Figure 2e). The samples at fixed φ (9 vol%) showed substantial decrease in NP surface coverage at lower f (blue trace, Figure 3b), however, only modest change in thermal conductivity. On the other hand, lowering φ with fixed f similarly decreased surface coverage (red trace, Figure 3b) but demonstrate significant reduction in thermal conductivity. The sensitivity to concentration rather than surface coverage verifies that percolation effect is not a consequence of NP accumulation at the surface. Note that TTG measurements in the transmission geometry, as performed in this study, account for the entire cross-section of the film. Furthermore, the relatively high thermal conductivity of nanocomposites despite having low surface coverage (blue trace, Figure 3b) confirms that the NPs assembly in 3 dimensions.

The inability of established EMA methods in describing the system in question has motivated us to develop a model using ideal constructs such as the thermal resistance circuits (Figure 3c). The nanocomposite is divided into two blocks connected in parallel, which consist of the PS and P4VP(PDP) blocks. In the latter block, a series circuit is embedded between the NPs and P4VP(PDP) matrix. Assuming heat transfer along both parallel and perpendicular to the two blocks, the overall thermal resistance of the composite can be described as a series embedded into a parallel circuit (SEP). The effective thermal conductivity, k_{eff} is given as a mixture of parallel and series circuit between NP embedded comb-block, $k_{NP\,block}$ and the surrounding polymer-block,

 $k_{matrix\ block}$ (Equation 1, Derived in the supporting information Section S3). $K_{NP\ block}$ comprises of several components including the NP core, k_{core} , ligand, k_L , PS-b-P4VP(PDP) polymer matrix, k_m , and the thermal conductance at both interfaces, h_{NL} and h_{Lm} (Details on each variable is provided in the supporting information Section S3). Note that bulk k values were used for the NP core, thus, size effects were not considered as it was previously demonstrated that the interface dominates conductivity at these length scales.⁴³ A is the volume fraction of the NP block and is taken as the point where percolation occurs, which in this case 9 vol%. This corroborates with the assemblies previously observed on this matrix.²⁴ Equation 1 can be written in terms of interparticle distance, D_{NP} by assuming NPs to be cylindrical in shape (solely for the purpose of converting φ to D_{NP}). Thus, volume fraction within the NP block can be expressed as $\emptyset = \frac{l}{D_{NP}}$ where l is the characteristic length of the component (Equation 2).

$$k_{eff} = \frac{1}{2} A_{\frac{\vartheta_{NP}}{k_{core}} + \frac{\vartheta_L}{k_L} + \frac{\vartheta_m}{k_m} + \frac{\vartheta_{NP}}{h_{NL}l_{NP}} + \frac{\vartheta_m}{h_{Lm}l_{NP}}} + (1 - A) k_{matrix \ block} \quad \text{Equation 1}$$

$$k_{eff} = \frac{1}{2} A_{\frac{l_{NP}}{k_{core}D_{NP}} + \frac{l_L}{k_LD_{NP}} + \frac{l_m}{k_{mDNP}} + \frac{l_m}{h_{ND}D_{NP}} + \frac{l_m}{h_{Lm}l_{NP}D_{NP}}}} + (1 - A) k_{matrix \ block} \qquad \text{Equation 2}$$

Using the SEP model, thermal conductivity can be calculated as function of interparticle distance rather than volume fraction, which narrows the dependence of effective thermal conductivity, k_{eff} , down to NP distance, D_{NP} . The interfacial thermal conductance h_{N-L} (NP-ligand, 140 MW/m² K)⁴³ along with k_{core} (6.05 W/m K)³⁵, k_{matrix} (0.1 W/m K)⁴⁴ and k_L (0.22 W/m K)⁴³ was obtained from literature while h_{L-M} (Ligand-matrix, 11 MW/m² K) was attained by fitting the data to the SEP model. H_{L-M} was found to be in excellent agreement with colloidal CNTs in polymer surfactants.⁴⁵ SEP, based on the phonon particle picture, works well for the nanocomposites likely because of weak coupling between the filler and matrix suppresses phonon coherence.⁴⁶

The effect of contrast ratio, k_f/k_m was investigated by varying k_{core} and keeping k_m constant (Figure 3d). Surprisingly, the model predicts that enhancements from thermal percolation at k_f/k_m = 60.5 (Fe₃O₄) is comparable to 10⁴ (equivalent of graphene). This result contradicts the long-standing view that high contrast ratio is required for thermal percolation to occur, largely due to the use of random composites. Nevertheless, the effects of percolation indeed tail off at $k_f/k_m \sim 10$, confirming the significance of contrast ratio, albeit several orders of magnitude lower than previously predicted. A significant difference between the model presented here and literature lies in the treatment of interfacial thermal conductance, which features two interfaces: nanoparticle-ligand, h_{N-L} and ligand-matrix, h_{L-M} . At the percolating threshold, h_{L-M} is eliminated reducing the interface to h_{N-L} since the ligand-ligand interface between NPs form excellent thermal contacts. Hence, corroboration between the data and model also highlights the role of ligands in mitigating filler-filler contact resistance—an artifact known to suppress thermal percolation.

The chemical compatibility between oleic acid ligands and P4VP(PDP) matrix facilitates the selective localization of NPs into a single microdomain. Interestingly, despite their chemical similarity, h_{L-M} is significantly lower than the NP-ligand and ligand-ligand interface. To gain further insight into the h_{L-M} interface, we turn to vibrational energy coupling, which facilitates phonon transfer between heterogeneous surfaces. 45-46, 49 We analyzed each chemical component present in the NP-P4VP(PDP) interface (Figure 3e) and generated their vibrational energy spectra through lattice dynamics calculations (Figure 3f, Details of the calculations are provided in the Supporting Information Section S4). At room temperature (25 meV), significant overlap among the accessible vibrational energies was observed between oleic acid (OA, NP ligand) and PDP, as expected from their analogous chemical structures. Similarly, the vibrational energy band of iron oxide (Fe₃O₄) peaks around this energy range. 50 In contrast, few active states are present in P4VP

repeat units because aromatic hydrocarbons tend to resonate at higher energies.⁵¹ Given the complexity of the ligand-polymer interface where the number of PDP-oleic acid contacts are limited by steric hindrance from the P4VP chains, the 4VP units could play a significant role at the boundary. Therefore, we attribute the poor conductance (h_{L-M}) to insufficient coupling of vibrational energy states at room temperature.

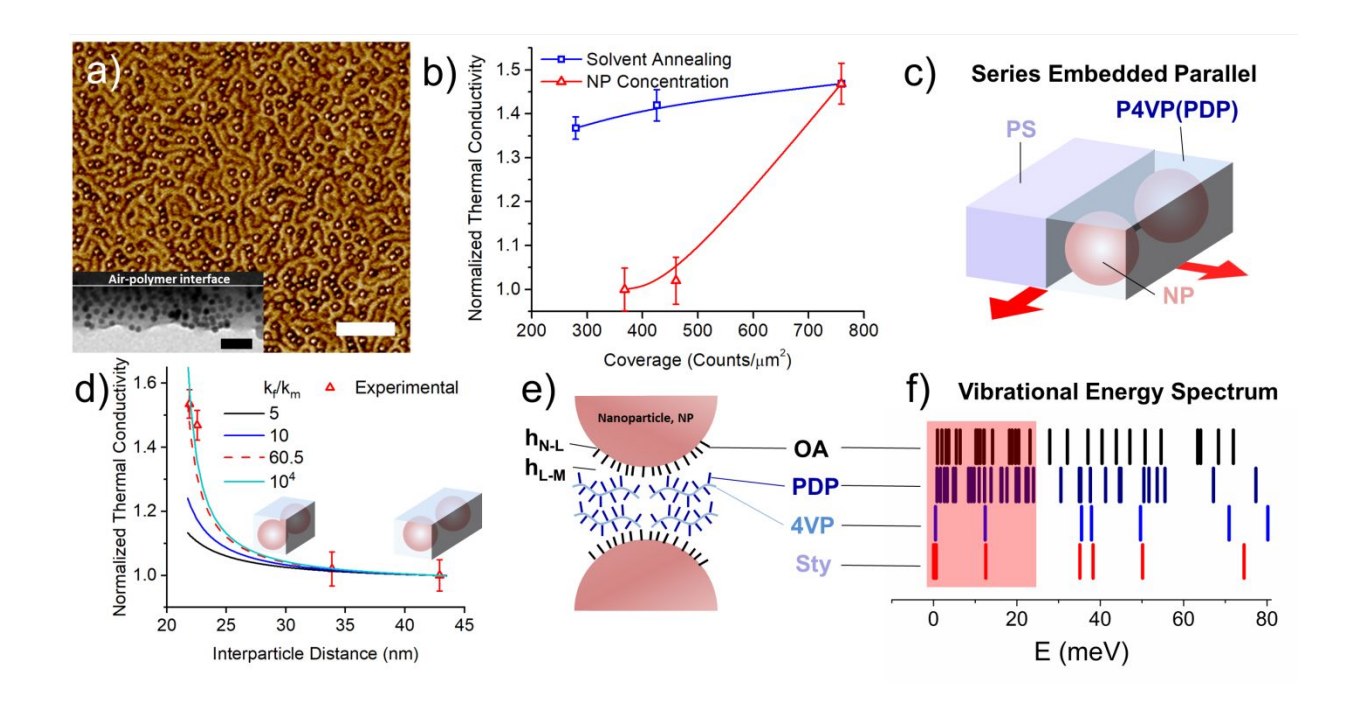


Figure 3. Structure-derived model and insights into the thermal conductivity contrast ratio k_f/k_m on thermal percolation. a) AFM image of nanocomposite with 20.4 nm NPs annealed to f=0.2. Inset shows a cross-section TEM the nanocomposite annealed to f=0.62. (Scale bar=200nm, Inset=100nm). b) Thermal conductivity as a function of NP surface coverage induced by solvent annealing (blue) and increasing NP concentration (red). Solid lines are drawn as a guide to the eye. c) Schematic representation of the series embedded parallel (SEP) model. d) Normalized thermal conductivity as a function of interparticle distance of the 20.4 nm nanocomposite and fitted SEP

model based on contrast ratio of Fe_3O_4 (60.5). The contrast ratio of fillers is varied assuming the same structure and interfacial conductance, h obtained from the fit. e) Schematic and f) vibrational energy spectrum of the components separating NPs in the comb block from lattice dynamics calculations. Red highlight represents active states at room temperature.

NP size is known to affect a multitude of properties such as band gap, mechanical strength and surface plasmon resonance. Percolated composites, however, is not well understood because of challenges in controlling structure of the nanocomposite. Studies have shown that filler size could shift percolating thresholds, which convolutes the effect of size with volume fraction. Thus, only computational methods have produced general relationships between size and thermal percolation. See Supramolecular nanocomposites can accommodate different NP sizes while maintaining selective placement into a single domain, serving as a model system for studying nanocomposite size effects. In general, filler size has two levels affecting thermal conductivity, i) interface density that amplifies interfacial resistance and ii) phonon boundary scattering when its mean free path, Λ is comparable to the filler size. The latter is important in highly conductive fillers such as graphene as thermal conductivity scales with Λ . Hence, the effects of boundary scattering are negligible here since the NP sizes sampled in this work maintains above the Λ of Fe₃O₄ (~1 nm from kinetic theory).

We fabricated nanocomposites with NP sizes, d between 5.6-25.7 nm with equal loading (9 vol%) and examined their morphology in AFM. At 5 nm, the nanocomposite exhibited similar morphology to the native supramolecule (Figure 4a-b). Systematic characterization of this hexagonal close packed (HCP) cylinder forming thin film revealed that NPs in this size regime reside within interstitial sites as they are significantly smaller than the BCP periodicity, L.^{22, 25}

Nanocomposites with 10.7 and 24.7 nm particles appeared more distorted (Figure 4c-d) similar to 20.4 nm (Figure 2c) because of size-induced entropic penalty at $d/L > 0.3.^{58-59}$ Similarly, the more pronounced disorder observed at 10.7 nm compared to larger NPs likely stem from its position at d/L~0.33, which is at the boundary of the morphological transition. Normalized thermal conductivity of the films were evaluated with EMA (Hasselman-Johnson) and SEP model (Figure 4e). The data showed excellent agreement with the SEP model between 10.7-25.7 nm, verifying that the nanocomposites at various filler sizes retain their percolating networks. The increase in thermal conductivity with size is a result of reduced number of interfaces and increasing fraction of the inorganic core along the percolating network. This is verified by the decay in interfacial resistivity with increasing NP size (Figure S7). The 5.6 nm composite, however, consists of more ordered chains, which can significantly improve the transmission of acoustic phonons due to larger mean free path and reduced scattering centers. 60-63 Furthermore, the tortuosity of the percolating networks in the 5.6 nm nanocomposite is significantly decreased through the formation of ordered grains. In general, the size-modified EMA underpredicts the effect of size on normalized thermal conductivity. This observation implies that percolated systems are more sensitive to NP size compared to randomly dispersed composites.

As discussed above, filler-filler interface scales with NP size and thus, plays a dominant role on heat transport along percolating networks. We further applied the SEP model to study the effects of interfacial thermal conductance (ITC), h_{N-L} and thermal conductivity contrast ratio, k_f/k_m with respect to NP size (Figure 4f-g). At low ITC (10MW/m²K), thermal transport becomes insensitive to NP size (Figure 4f). This result has significant implications as van der Waals bonded matrix-filler interfaces, which represent the most common type of polymer composite fall into under this regime.^{45, 64} Hence, despite the formation of networks, thermal percolation is unlikely

to occur when the filler is weakly bonded to the organic phase. Simulations have shown, however, that enhancing intermolecular interactions with hydrogens bonds could significantly improve thermal conductivity. 65-66

At high contrast ratios, thermal conductivity increases linearly with NP size, which is a direct result of depleting interfaces (Figure 4g). We begin to observe saturated enhancements at k_f/k_m =60.5 (Fe₃O₄) albeit maintaining a substantial increase in thermal conductivity with size, once again highlighting that thermal percolation is not exclusive to highly conductive fillers such as graphene (k_f/k_m =10⁵). Furthermore, common semiconducting NPs such as PbS and CdSe also fall into k_f/k_m =60.5, making percolating networks a viable solution for thermal management in NP based devices.

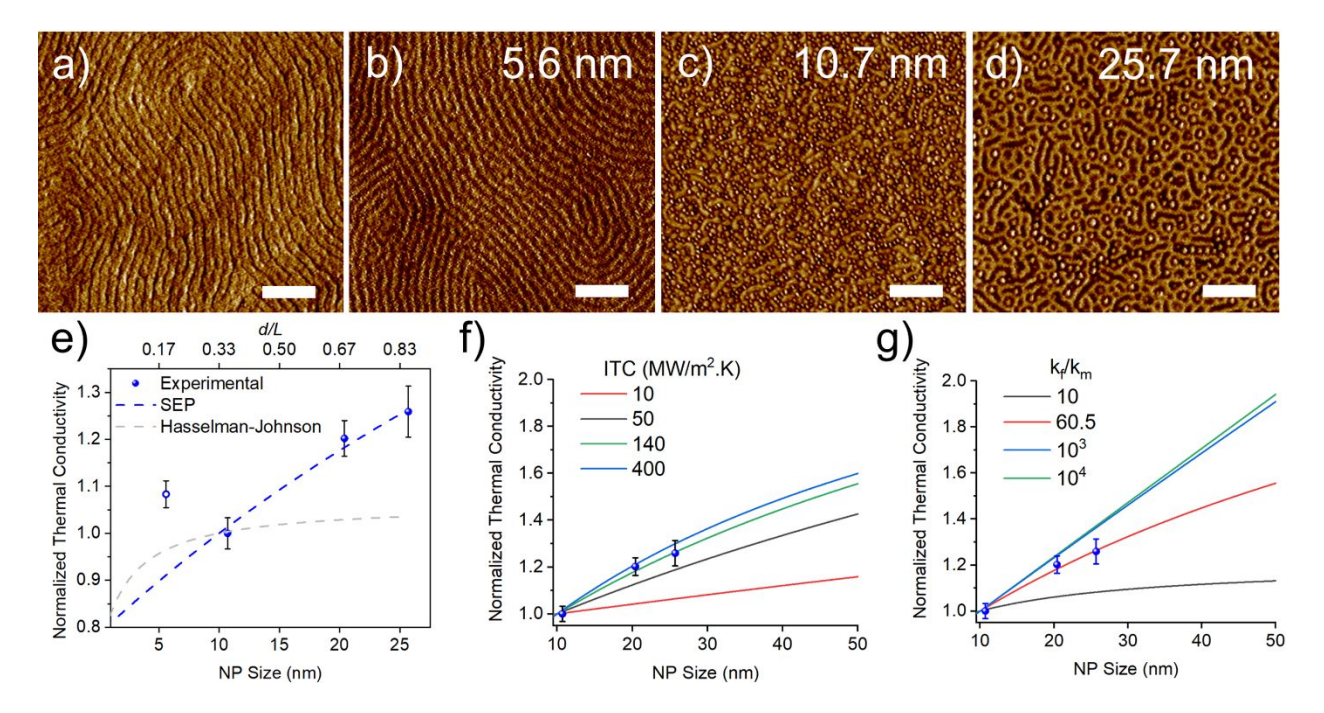


Figure 4. Effect of nanoparticle, NP size on thermal percolation. a) AFM images of the native supramolecule and b-d) 9% nanocomposite with varying NP size. e) Normalized thermal conductivity as a function of NP size, d and d to BCP periodicity, L ratio. The data is normalized

with respect to 10.7 nm given the distinctive morphology in the 5.6 nm nanocomposite. f-g) Impact of NP-ligand interfacial thermal conductance, h_{N-L} and contrast ratio on the size dependence of thermal conductivity (Parameters for the Fe₃O₄ NPs used: ITC=140 W/m.K, k_f/k_m = 60.5).

Conclusion

In conclusion, we reveal the general properties of thermal percolated nanocomposites using a self-assembled matrix as a model system with a well-defined morphology. This work demonstrates that thermal percolation is not limited to high contrast ratio, k_f/k_m systems such as CNT and graphene. In fact, k_f/k_m plays a minor role above 60.5, which is the common range for NP-based semiconductors, highlighting thermal percolation as a feasible route for thermal management in nanocomposite devices. Furthermore, the effect of percolation is strongly governed by the filler-filler interfaces. Thermal transport is compromised when the fillers are weakly bonded to the organic phase within the networks because of low interfacial thermal conductance. Finally, thermal conductivity increases with filler size in when $k_f/k_m > 60$ due to depleting interfaces. While at $k_f/k_m \sim 10$, the lack of contrast renders thermal conductivity insensitive to filler size. This work provides new insight into the limits of thermal percolation in nanocomposites where this method of thermal management could be extended to general fillers relevant to semiconducting and other multifunctional devices.

Associated Content

Supporting information

The Supporting Information is available free of charge at

Detailed information on experimental methods, materials, SEP model and vibrational energy calculations and substrate effect calculations.

Author Information

Corresponding Author

Ting Xu – Department of Materials Science and Engineering, University of California–Berkeley, Berkeley, California 94720, United States; Materials Sciences Division, Lawrence Berkeley National Lab, Berkeley, California 94720, United States. Email: tingxu@berkeley.edu

Zhiting Tian – Sibley School of Mechanical and Aerospace Engineering, Cornell University,

Ithaca, New York 14853, United States. Email: zhiting@cornell.edu

Author Contributions

B.C. and C.L. contributed equally. The manuscript was written through contributions of all authors.

Notes

The authors declare no conflict of interest.

Acknowledgements

This work was funded by the U.S. Department of Energy, Office of Science, Office of Basic Energy Sciences, Materials Sciences and Engineering Division, under Contract DE-AC02-05-CH11231 (Organic–Inorganic Nanocomposites KC3104). Z.T., C.L., and J.D. acknowledge the support by NSF CAREER Award (CBET-1839384).

References

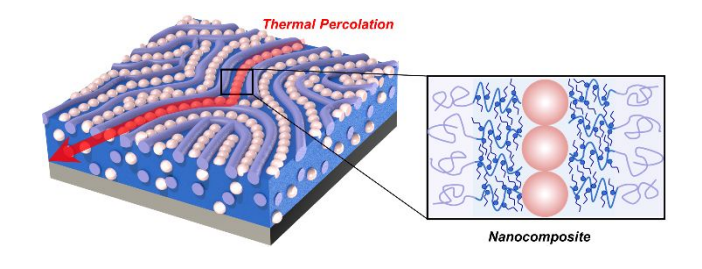
- 1. Balazs, A. C.; Emrick, T.; Russell, T. P., Nanoparticle Polymer Composites: Where Two Small Worlds Meet. *Science* **2006**, *314* (5802), 1107.
- 2. Huang, C.; Qian, X.; Yang, R., Thermal conductivity of polymers and polymer nanocomposites. *Materials Science and Engineering: R: Reports* **2018**, *132*, 1-22.
- 3. Chen, H.; Ginzburg, V. V.; Yang, J.; Yang, Y.; Liu, W.; Huang, Y.; Du, L.; Chen, B., Thermal conductivity of polymer-based composites: Fundamentals and applications. *Progress in Polymer Science* **2016**, *59*, 41-85.
- 4. Ahn, C.; Kim, S.-M.; Jung, J.-W.; Park, J.; Kim, T.; Lee, S. E.; Jang, D.; Hong, J.-W.; Han, S. M.; Jeon, S., Multifunctional Polymer Nanocomposites Reinforced by 3D Continuous Ceramic Nanofillers. *ACS Nano* **2018**, *12* (9), 9126-9133.
- 5. Acauan, L. H.; Zhou, Y.; Kalfon-Cohen, E.; Fritz, N. K.; Wardle, B. L., Multifunctional nanocomposite structural separators for energy storage. *Nanoscale* **2019**, *11* (45), 21964-21973.
- 6. Bockstaller, M. R.; Thomas, E. L., Optical Properties of Polymer-Based Photonic Nanocomposite Materials. *The Journal of Physical Chemistry B* **2003**, *107* (37), 10017-10024.
- 7. Patti, A.; Russo, P.; Acierno, D.; Acierno, S., The effect of filler functionalization on dispersion and thermal conductivity of polypropylene/multi wall carbon nanotubes composites. *Composites Part B: Engineering* **2016**, *94*, 350-359.
- 8. Shahil, K. M. F.; Balandin, A. A., Graphene–Multilayer Graphene Nanocomposites as Highly Efficient Thermal Interface Materials. *Nano Letters* **2012**, *12* (2), 861-867.
- 9. Song, W.-L.; Wang, P.; Cao, L.; Anderson, A.; Meziani, M. J.; Farr, A. J.; Sun, Y.-P., Polymer/Boron Nitride Nanocomposite Materials for Superior Thermal Transport Performance. *Angewandte Chemie International Edition* **2012**, *51* (26), 6498-6501.
- 10. Garimella, S. V.; Fleischer, A. S.; Murthy, J. Y.; Keshavarzi, A.; Prasher, R.; Patel, C.; Bhavnani, S. H.; Venkatasubramanian, R.; Mahajan, R.; Joshi, Y.; Sammakia, B.; Myers, B. A.; Chorosinski, L.; Baelmans, M.; Sathyamurthy, P.; Raad, P. E., Thermal Challenges in Next-Generation Electronic Systems. *IEEE Transactions on Components and Packaging Technologies* **2008**, *31* (4), 801-815.
- 11. Chang, B.; Zhong, L.; Akinc, M., Low cost composites for vacuum insulation core material. *Vacuum* **2016**, *131*, 120-126.
- 12. Snyder, G. J.; Toberer, E. S., Complex thermoelectric materials. In *Materials for Sustainable Energy*, Co-Published with Macmillan Publishers Ltd, UK: 2010; pp 101-110.
- 13. Dresselhaus, M. S.; Chen, G.; Tang, M. Y.; Yang, R. G.; Lee, H.; Wang, D. Z.; Ren, Z. F.; Fleurial, J. P.; Gogna, P., New Directions for Low-Dimensional Thermoelectric Materials. *Advanced Materials* **2007**, *19* (8), 1043-1053.
- 14. Shenogina, N.; Shenogin, S.; Xue, L.; Keblinski, P., On the lack of thermal percolation in carbon nanotube composites. *Applied Physics Letters* **2005**, *87* (13), 133106.
- 15. Li, A.; Zhang, C.; Zhang, Y.-F., Graphene nanosheets-filled epoxy composites prepared by a fast dispersion method. *Journal of Applied Polymer Science* **2017**, *134* (36), 45152.
- 16. Shtein, M.; Nadiv, R.; Buzaglo, M.; Kahil, K.; Regev, O., Thermally Conductive Graphene-Polymer Composites: Size, Percolation, and Synergy Effects. *Chemistry of Materials* **2015**, *27* (6), 2100-2106.

- 17. Kargar, F.; Barani, Z.; Salgado, R.; Debnath, B.; Lewis, J. S.; Aytan, E.; Lake, R. K.; Balandin, A. A., Thermal Percolation Threshold and Thermal Properties of Composites with High Loading of Graphene and Boron Nitride Fillers. *ACS Applied Materials & Interfaces* **2018**, *10* (43), 37555-37565.
- 18. Gurijala, A.; Zando, R. B.; Faust, J. L.; Barber, J. R.; Zhang, L.; Erb, R. M., Castable and Printable Dielectric Composites Exhibiting High Thermal Conductivity via Percolation-Enabled Phonon Transport. *Matter* **2020**, *2* (4), 1015-1024.
- 19. Barani, Z.; Mohammadzadeh, A.; Geremew, A.; Huang, C.-Y.; Coleman, D.; Mangolini, L.; Kargar, F.; Balandin, A. A., Thermal Properties of the Binary-Filler Hybrid Composites with Graphene and Copper Nanoparticles. *Advanced Functional Materials* **2020**, *30* (8), 1904008.
- 20. Bonnet, P.; Sireude, D.; Garnier, B.; Chauvet, O., Thermal properties and percolation in carbon nanotube-polymer composites. *Applied Physics Letters* **2007**, *91* (20), 201910.
- 21. Zhao, Y.; Thorkelsson, K.; Mastroianni, A. J.; Schilling, T.; Luther, J. M.; Rancatore, B. J.; Matsunaga, K.; Jinnai, H.; Wu, Y.; Poulsen, D.; Fréchet, J. M. J.; Paul Alivisatos, A.; Xu, T., Small-molecule-directed nanoparticle assembly towards stimuli-responsive nanocomposites. *Nat. Mater.* **2009**, *8* (12), 979-985.
- 22. Kao, J.; Bai, P.; Chuang, V. P.; Jiang, Z.; Ercius, P.; Xu, T., Nanoparticle Assemblies in Thin Films of Supramolecular Nanocomposites. *Nano Letters* **2012**, *12* (5), 2610-2618.
- 23. Huang, J.; Qian, Y.; Evans, K.; Xu, T., Diffusion-Dependent Nanoparticle Assembly in Thin Films of Supramolecular Nanocomposites: Effects of Particle Size and Supramolecular Morphology. *Macromolecules* **2019**, *52* (15), 5801-5810.
- 24. Kao, J.; Xu, T., Nanoparticle Assemblies in Supramolecular Nanocomposite Thin Films: Concentration Dependence. *J. Am. Chem. Soc.* **2015**, *137* (19), 6356-6365.
- 25. Kao, J.; Bai, P.; Lucas, J. M.; Alivisatos, A. P.; Xu, T., Size-Dependent Assemblies of Nanoparticle Mixtures in Thin Films. *Journal of the American Chemical Society* **2013**, *135* (5), 1680-1683.
- 26. Chang, B. S.; Ma, L.; He, M.; Xu, T., NMR Studies of Block Copolymer-Based Supramolecules in Solution. *Acs Macro Lett* **2020**, *9* (7), 1060-1066.
- 27. Evans, K.; Xu, T., Self-Assembly of Supramolecular Thin Films: Role of Small Molecule and Solvent Vapor Annealing. *Macromolecules* **2019**, *52* (2), 639-648.
- 28. Huang, J.; Xiao, Y.; Xu, T., Achieving 3-D Nanoparticle Assembly in Nanocomposite Thin Films via Kinetic Control. *Macromolecules* **2017**, *50* (5), 2183-2188.
- 29. Li, C.; Ma, Y.; Tian, Z., Thermal Switching of Thermoresponsive Polymer Aqueous Solutions. *Acs Macro Lett* **2018**, *7* (1), 53-58.
- 30. Xia, S.; Song, L.; Körstgens, V.; Opel, M.; Schwartzkopf, M.; Roth, S. V.; Müller-Buschbaum, P., Magnetic nanoparticle-containing soft—hard diblock copolymer films with high order. *Nanoscale* **2018**, *10* (25), 11930-11941.
- 31. Kao, J.; Tingsanchali, J.; Xu, T., Effects of Interfacial Interactions and Film Thickness on Nonequilibrium Hierarchical Assemblies of Block Copolymer-Based Supramolecules in Thin Films. *Macromolecules* **2011**, *44* (11), 4392-4400.
- 32. Kao, J.; Thorkelsson, K.; Bai, P.; Zhang, Z.; Sun, C.; Xu, T., Rapid fabrication of hierarchically structured supramolecular nanocomposite thin films in one minute. *Nat. Commun.* **2014,** *5* (1), 4053.
- 33. Kao, J.; Jeong, S.-J.; Jiang, Z.; Lee, D. H.; Aissou, K.; Ross, C. A.; Russell, T. P.; Xu, T., Direct 3-D Nanoparticle Assemblies in Thin Films via Topographically Patterned Surfaces. *Advanced Materials* **2014**, *26* (18), 2777-2781.
- 34. Yuan, C.; Duan, B.; Li, L.; Xie, B.; Huang, M.; Luo, X., Thermal Conductivity of Polymer-Based Composites with Magnetic Aligned Hexagonal Boron Nitride Platelets. *ACS Applied Materials & Interfaces* **2015**, *7* (23), 13000-13006.

- 35. Chi, Q.; Ma, T.; Dong, J.; Cui, Y.; Zhang, Y.; Zhang, C.; Xu, S.; Wang, X.; Lei, Q., Enhanced Thermal Conductivity and Dielectric Properties of Iron Oxide/Polyethylene Nanocomposites Induced by a Magnetic Field. *Scientific Reports* **2017**, *7* (1), 3072.
- 36. Johnson, J. A.; Maznev, A. A.; Bulsara, M. T.; Fitzgerald, E. A.; Harman, T. C.; Calawa, S.; Vineis, C. J.; Turner, G.; Nelson, K. A., Phase-controlled, heterodyne laser-induced transient grating measurements of thermal transport properties in opaque material. *Journal of Applied Physics* **2012**, *111* (2), 023503.
- 37. Nan, C.; Shen, Y.; Ma, J., Physical properties of composites near percolation. *Annual Review of Materials Research* **2010**, *40* (1), 131-151.
- 38. Ma, P.-C.; Siddiqui, N. A.; Marom, G.; Kim, J.-K., Dispersion and functionalization of carbon nanotubes for polymer-based nanocomposites: A review. *Composites Part A: Applied Science and Manufacturing* **2010**, *41* (10), 1345-1367.
- 39. Yu, A.; Ramesh, P.; Sun, X.; Bekyarova, E.; Itkis, M. E.; Haddon, R. C., Enhanced Thermal Conductivity in a Hybrid Graphite Nanoplatelet Carbon Nanotube Filler for Epoxy Composites. *Advanced Materials* **2008**, *20* (24), 4740-4744.
- 40. Hasselman, D. P. H.; Johnson, L. F., Effective Thermal Conductivity of Composites with Interfacial Thermal Barrier Resistance. *Journal of Composite Materials* **1987**, *21* (6), 508-515.
- 41. Nan, C.-W.; Birringer, R.; Clarke, D. R.; Gleiter, H., Effective thermal conductivity of particulate composites with interfacial thermal resistance. *Journal of Applied Physics* **1997**, *81* (10), 6692-6699.
- 42. Yang, X.; Hu, J.; Chen, S.; He, J., Understanding the Percolation Characteristics of Nonlinear Composite Dielectrics. *Scientific Reports* **2016**, *6* (1), 30597.
- 43. Ong, W.-L.; Rupich, S. M.; Talapin, D. V.; McGaughey, A. J. H.; Malen, J. A., Surface chemistry mediates thermal transport in three-dimensional nanocrystal arrays. *Nature Materials* **2013**, *12* (5), 410-415.
- 44. Mark, J. E., *Polymer Data Handbook*. Oxford University Press: 1999. pp. 834.
- 45. Huxtable, S. T.; Cahill, D. G.; Shenogin, S.; Xue, L.; Ozisik, R.; Barone, P.; Usrey, M.; Strano, M. S.; Siddons, G.; Shim, M.; Keblinski, P., Interfacial heat flow in carbon nanotube suspensions. *Nature Materials* **2003**, *2* (11), 731-734.
- 46. Deng, C.; Huang, Y.; An, M.; Yang, N., Phonon weak couplings model and its applications: A revisit to two-temperature non-equilibrium transport. *Materials Today Physics* **2021**, *16*, 100305.
- 47. Kumar, S.; Alam, M. A.; Murthy, J. Y., Effect of percolation on thermal transport in nanotube composites. *Applied Physics Letters* **2007**, *90* (10), 104105.
- 48. Kaur, S.; Raravikar, N.; Helms, B. A.; Prasher, R.; Ogletree, D. F., Enhanced thermal transport at covalently functionalized carbon nanotube array interfaces. *Nature Communications* **2014**, *5* (1), 3082.
- 49. Sun, F.; Zhang, T.; Jobbins, M. M.; Guo, Z.; Zhang, X.; Zheng, Z.; Tang, D.; Ptasinska, S.; Luo, T., Molecular Bridge Enables Anomalous Enhancement in Thermal Transport across Hard-Soft Material Interfaces. *Advanced Materials* **2014**, *26* (35), 6093-6099.
- 50. Handke, B.; Kozłowski, A.; Parliński, K.; Przewoźnik, J.; Ślęzak, T.; Chumakov, A. I.; Niesen, L.; Kąkol, Z.; Korecki, J., Experimental and theoretical studies of vibrational density of states in Fe3O4 single-crystalline thin films. *Physical Review B* **2005**, *71* (14), 144301.
- 51. Pivovar, A. M.; Curtis, J. E.; Leao, J. B.; Chesterfield, R. J.; Frisbie, C. D., Structural and vibrational characterization of the organic semiconductor tetracene as a function of pressure and temperature. *Chemical Physics* **2006**, *325* (1), 138-151.
- 52. Satoh, N.; Nakashima, T.; Kamikura, K.; Yamamoto, K., Quantum size effect in TiO2 nanoparticles prepared by finely controlled metal assembly on dendrimer templates. *Nature Nanotechnology* **2008**, *3* (2), 106-111.
- 53. An, L.; Zhang, D.; Zhang, L.; Feng, G., Effect of nanoparticle size on the mechanical properties of nanoparticle assemblies. *Nanoscale* **2019**, *11* (19), 9563-9573.

- 54. Campos, A.; Troc, N.; Cottancin, E.; Pellarin, M.; Weissker, H.-C.; Lermé, J.; Kociak, M.; Hillenkamp, M., Plasmonic quantum size effects in silver nanoparticles are dominated by interfaces and local environments. *Nature Physics* **2019**, *15* (3), 275-280.
- 55. Devpura, A.; Phelan, P. E.; Prasher, R. S., Size Effects on the Thermal Conductivity of Polymers Laden with Highly Conductive Filler Particles. *Microscale Thermophysical Engineering* **2001**, *5* (3), 177-189.
- 56. Tian, W.; Yang, R., Effect of interface scattering on phonon thermal conductivity percolation in random nanowire composites. *Applied Physics Letters* **2007**, *90* (26), 263105.
- 57. Tian, W.; Yang, R., Phonon Transport and Thermal Conductivity Percolation in Random Nanoparticle Composites. *Computer Modeling in Engineering* \& *Sciences* **2008**, *24* (2&3).
- 58. Thompson, R. B.; Ginzburg, V. V.; Matsen, M. W.; Balazs, A. C., Predicting the Mesophases of Copolymer-Nanoparticle Composites. *Science* **2001**, *292* (5526), 2469.
- 59. Bockstaller, M. R.; Lapetnikov, Y.; Margel, S.; Thomas, E. L., Size-Selective Organization of Enthalpic Compatibilized Nanocrystals in Ternary Block Copolymer/Particle Mixtures. *Journal of the American Chemical Society* **2003**, *125* (18), 5276-5277.
- 60. Shen, S.; Henry, A.; Tong, J.; Zheng, R.; Chen, G., Polyethylene nanofibres with very high thermal conductivities. *Nature Nanotechnology* **2010**, *5* (4), 251-255.
- 61. Liu, J.; Yang, R., Tuning the thermal conductivity of polymers with mechanical strains. *Physical Review B* **2010**, *81* (17), 174122.
- 62. Ma, H.; Tian, Z., Chain rotation significantly reduces thermal conductivity of single-chain polymers. *Journal of Materials Research* **2018**, *34* (1), 126-133.
- 63. Ma, H.; O'Donnel, E.; Tian, Z., Tunable thermal conductivity of π -conjugated two-dimensional polymers. *Nanoscale* **2018**, *10* (29), 13924-13929.
- 64. Losego, M. D.; Grady, M. E.; Sottos, N. R.; Cahill, D. G.; Braun, P. V., Effects of chemical bonding on heat transport across interfaces. *Nature Materials* **2012**, *11* (6), 502-506.
- 65. Deng, S.; Ma, D.; Zhang, G.; Yang, N., Modulating the thermal conductivity of crystalline nylon by tuning hydrogen bonds through structure poling. *Journal of Materials Chemistry A* **2021**, *9* (43), 24472-24479.
- 66. Ma, H.; Li, C.; Tian, Z., Hydrogen Bonds Significantly Enhance Out-of-Plane Thermal and Electrical Transport in 2D Graphamid: Implications for Energy Conversion and Storage. *ACS Applied Nano Materials* **2020**, *3* (11), 11090-11097.

TOC



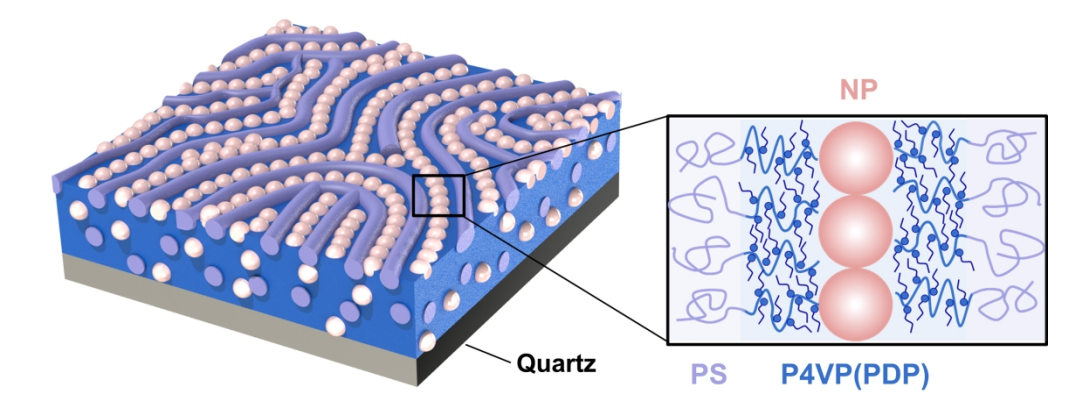


Figure 1. Schematic of bottom-up assembled block copolymer-based supramolecular nanocomposite. The supramolecule self-assembles into a cylindrical morphology isolating the nanoparticles (NP) to form a percolating network within the P4VP(PDP) domain.

165x62mm (400 x 400 DPI)

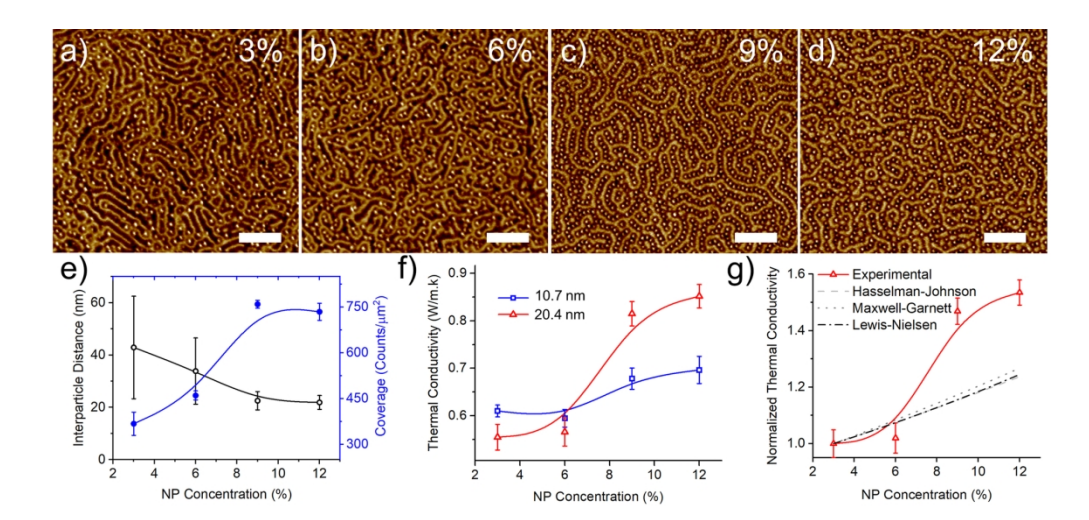


Figure 2. Morphology and thermal conductivity of a percolating nanocomposite through self-assembly. a-d) AFM images of nanocomposites with 20.4 nm NPs at various concentrations. Nanocomposite lateral periodicity, L = 45nm (Scale bar=200nm). E) Average interparticle distance and NP surface coverage from image processing of AFM images, and f) thermal conductivity as a function of NP concentration. g) Normalized thermal conductivity with respect to 3 vol% compared to effective medium approximation by Maxwell-Garnett and the inclusion size corrected Hasselman-Johnson model. Solid lines are drawn as a guide to the eye.

164x78mm (300 x 300 DPI)

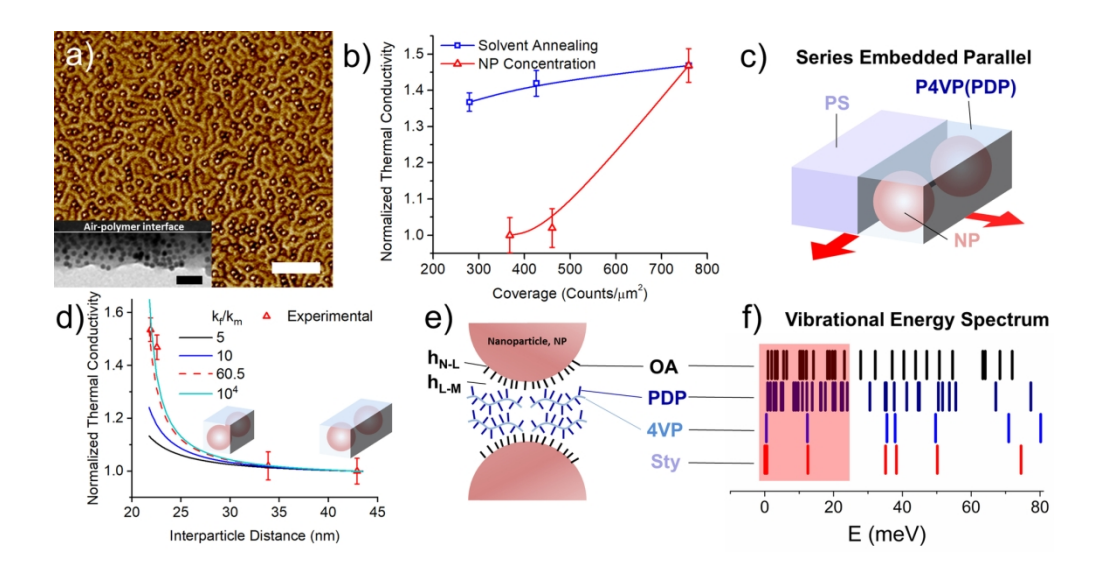


Figure 3. Structure-derived model and insights into the thermal conductivity contrast ratio k_f/k_m on thermal percolation. a) AFM image of nanocomposite with 20.4 nm NPs annealed to f=0.2. Inset shows a crosssection TEM the nanocomposite annealed to f=0.62. (Scale bar=200nm, Inset=100nm). b) Thermal conductivity as a function of NP surface coverage induced by solvent annealing (blue) and increasing NP concentration (red). Solid lines are drawn as a guide to the eye. c) Schematic representation of the series embedded parallel (SEP) model. d) Normalized thermal conductivity as a function of interparticle distance of the 20.4 nm nanocomposite and fitted SEP model based on contrast ratio of Fe₃O₄ (60.5). The contrast ratio of fillers is varied assuming the same structure and interfacial conductance, h obtained from the fit. e) Schematic and f) vibrational energy spectrum of the components separating NPs in the comb block from lattice dynamics calculations. Red highlight represents active states at room temperature.

165x85mm (300 x 300 DPI)

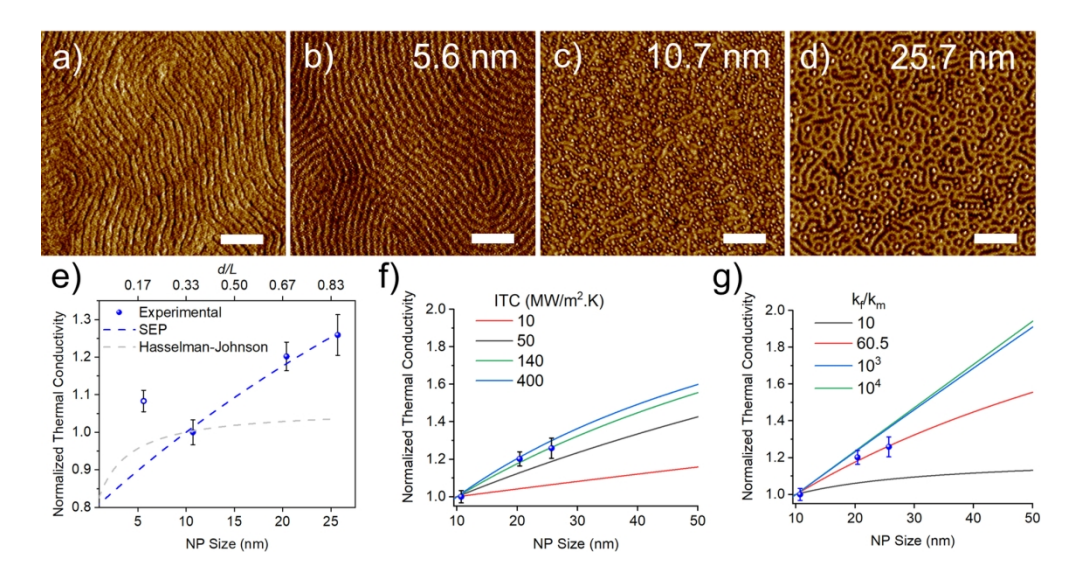
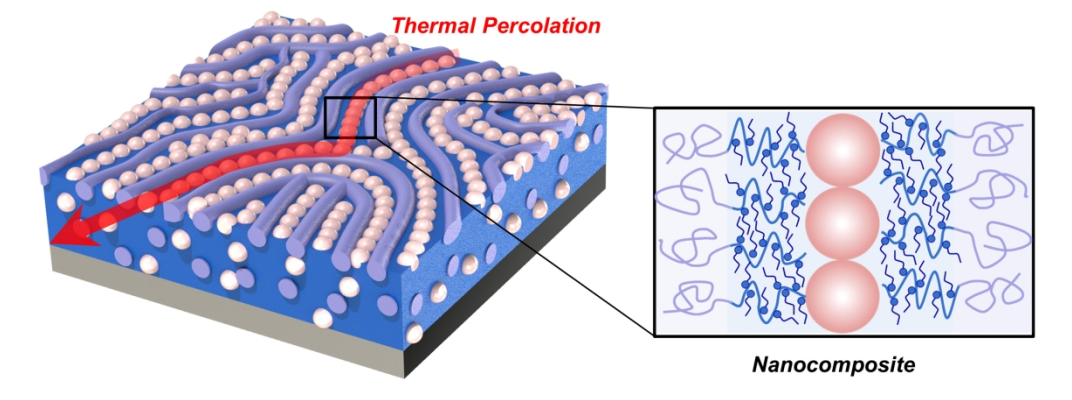


Figure 4. Effect of nanoparticle, NP size on thermal percolation. a) AFM images of the native supramolecule and b-d) 9% nanocomposite with varying NP size. e) Normalized thermal conductivity as a function of NP size, d and d to BCP periodicity, L ratio. The data is normalized with respect to 10.7 nm given the distinctive morphology in the 5.6 nm nanocomposite. f-g) Impact of NP-ligand interfacial thermal conductance, h_{N-L} and contrast ratio on the size dependence of thermal conductivity (Parameters for the Fe₃O₄ NPs used: ITC=140 W/m.K, $k_{\rm f}/k_{\rm m}=60.5$).

165x86mm (300 x 300 DPI)



TOC

82x30mm (800 x 800 DPI)